

# Myoglobin as a model system for designing heme protein based blood substitutes

Yi Dou<sup>a,b,1</sup>, David H. Mailliet<sup>a,b</sup>, Raymund F. Eich<sup>a,b,2</sup>, John S. Olson<sup>a,b,\*</sup>

<sup>a</sup>Department of Biochemistry and Cell Biology, Rice University, Houston, TX 77005, USA

<sup>b</sup>W.M. Keck Center for Computational Biology, Rice University, Houston, TX 77005, USA

Received 13 September 2001; received in revised form 19 December 2001; accepted 19 December 2001

## Abstract

The ligand binding properties and resistances to denaturation of >300 different site-directed mutants of sperm whale, pig, and human myoglobin have been examined over the past 15 years. This library of recombinant proteins has been used to derive chemical mechanisms for ligand binding and to examine the factors governing holo- and apoglobin stability. We have also examined the effects of mutagenesis on the dioxygenation of NO by MbO<sub>2</sub> to form NO<sub>3</sub><sup>-</sup> and metMb. This reaction rapidly detoxifies NO and is a key physiological function of both myoglobins and hemoglobins. The mechanisms derived for O<sub>2</sub> binding and NO dioxygenation have been used to design safer, more efficient, and more stable heme protein-prototypes for use as O<sub>2</sub> delivery pharmaceuticals in transfusion therapy (i.e. blood substitutes). An interactive database is being developed (<http://olsonnt1.bioc.rice.edu/web/myoglobinhome.asp>) to allow rapid access to the ligand binding parameters, stability properties, and crystal structures of the entire set of recombinant myoglobins. The long-range goal is to use this library for developing general protein engineering principles and for designing individual heme proteins for specific pharmacological and industrial uses. © 2002 Elsevier Science B.V. All rights reserved.

**Keywords:** Mb engineering; Heme proteins; Blood substitutes

## 1. Introduction

Mammalian myoglobin functions as a storage

protein in striated muscle to provide a continuous supply of O<sub>2</sub> to the terminal mitochondrial oxidase. During muscle relaxation, red blood cells circulating through capillary beds provide O<sub>2</sub> for both oxidative phosphorylation and oxygenation of myoglobin. During contraction, blood flow is interrupted and O<sub>2</sub> is supplied to the mitochondria by release from myoglobin. In order to perform this storage–delivery function, myoglobin has evolved a relatively high affinity for O<sub>2</sub>. It has a P<sub>50</sub> or K<sub>d</sub> ≈ 1 μM, which is intermediate between that of

\*Corresponding author. Department of Biochemistry and Cell Biology, MS 140, Rice University, 6100 S. Main, Houston, TX 77005, USA. Tel.: +1-713-348-4910; fax: +1-713-348-5154.

E-mail address: [olson@rice.edu](mailto:olson@rice.edu) (J.S. Olson).

<sup>1</sup> Present address: Tanox, Inc., 10301 Stella Link Rd., Suite 500, Houston, TX 77025, USA.

<sup>2</sup> Present address: Williams Morgan & Amerson, 7676 Hillmont, Ste. 250, Houston, TX 77040, USA.

hemoglobin in red cells ( $P_{50} \approx 20\text{--}30 \mu\text{M}$ ) and the  $K_M$  of cytochrome *c* oxidase ( $\sim 0.01 \mu\text{M}$ ). Myoglobin discriminates in favor of  $\text{O}_2$  binding and against CO binding in order to function in the presence of the low levels of carbon monoxide that are produced as a result of heme catabolism, neuronal function, and cell signaling [1]. Oxy-myoglobin also serves to detoxify NO by rapidly oxidizing it to nitrate [2–4]. Brunori and others have argued that this function is required to prevent NO inhibition of both aconitase and cytochrome oxidase activity in myocytes and in the last year has promoted the idea that myoglobin is a ‘pseudo-enzymatic’ scavenger of nitric oxide [5–7]. Oxy-hemoglobin has been shown to perform a similar detoxification function for inhaled nitric oxide [8].

Between 1985 and 1994, five groups developed vectors for expressing large quantities of recombinant human hemoglobin and human, sperm whale, pig, and horse heart myoglobins in *Escherichia coli* [9–13]. These expression systems have been used to construct site-directed mutants that are designed to evaluate the structural factors that regulate  $\text{O}_2$  affinity, ligand discrimination, autooxidation, and the rate constants for oxygen association and disassociation (for an early review see Springer et al. [14]). This approach has also been used to examine the oxidative reaction of NO with  $\text{MbO}_2$  and  $\text{HbO}_2$ . A summary of the mechanisms for  $\text{O}_2$  binding and NO dioxygenation are presented in the first part of Section 3.

Mutagenesis approaches have also been used to determine the factors that govern holomyoglobin denaturation, heme loss, apoglobin unfolding and expression levels of intact myoglobin in *E. coli* [15–20]. These stability studies led to the development of Mb-based reagents for measuring the rate of heme loss from holoproteins (i.e. see [21,22]).

Our work on the mutagenesis of myoglobin has been driven strongly by commercial development of extracellular hemoglobin as a blood substitute. The library of structural and functional data for the Mb mutants has served as a resource for developing general heme protein engineering strategies and algorithms for optimizing multiple properties in product candidates. The major side effects of extracellular hemoglobins are blood pressure

elevation, vascular lesions, and gastrointestinal dysmotility [23–26]. We and the group at Baxter Hemoglobin Therapeutics have argued that all of these side effects are due to interference with NO signaling pathways [18,27–29]. Using the mechanism of NO dioxygenation as a guide, we were able to design Mb prototypes with 20-fold lower rates of NO scavenging. These ideas were transferred to Baxter Hemoglobin Therapeutics (formerly Somatogen, Inc.) for testing in vivo, using recombinant human hemoglobins with the same sets of mutations [3,28]. A similar strategy for reducing the NO reactivity of recombinant human hemoglobin has been reported by Brunori’s group [30]. The  $\text{O}_2$  transport properties of these mutants have to be optimized by second site replacements in order to increase  $\text{O}_2$  release rates and decrease  $\text{O}_2$  affinity. The strategies for reducing NO scavenging and for increasing  $\text{O}_2$  transport are presented in the second half of Section 3. The compromises and problems involved in the design and production of heme protein-based blood substitutes are presented in Section 4.

## 2. Methods

### 2.1. Recombinant myoglobin expression systems

Three different strategies have been used to express mammalian myoglobins in *E. coli*. The first strategy was based on methods developed by Nagai’s group to express and reconstitute the subunits of human hemoglobin [9]. Boxer’s group used this strategy to express human myoglobin as a fusion protein with the N-terminal 31 amino acids of cII, a regulatory protein of  $\lambda$  phage [10]. This fusion protein system was also used by Wilkinson’s group to produce recombinant pig myoglobin [12] and by Ikeda-Saito, Yi Dou, and coworkers to produce sperm whale myoglobins with an N-terminal Val residue [31]. In this system, the protein is expressed in inclusion bodies, solubilized, reconstituted with heme, and then the leader sequence cleaved with trypsin or Factor Xa.

The second system was developed by Springer and Sligar [11] and involves constitutive expression of sperm whale holomyoglobin from a plasmid containing the myoglobin gene plus the codon

Table 1

Ligand binding and NO-induced oxidation parameters for position 29(B10), 64(E7), and 68(E11) mutants of sperm whale myoglobin at pH 7, 20 °C

Myoglobin	$k'_{\text{O}_2}$ ( $\mu\text{M}^{-1} \text{s}^{-1}$ )	$k_{\text{O}_2}$ ( $\text{s}^{-1}$ )	$1/K_{\text{O}_2}$ ( $P_{50}$ ) ( $\mu\text{M}$ )	$k'_{\text{NO,ox}}$ ( $\mu\text{M}^{-1} \text{s}^{-1}$ )
Wild-type	17	15	0.91	34
H64Q	24	130	5.4	~60 <sup>a</sup>
H64F	75	10,000	130	60
L29F	21	1.4	0.067	8.1
L29W	0.25	8.5	34	3.2
V68I	3.2	14	4.4	33
V68L	23	6.8	0.30	24
V68F	1.2	2.5	2.1	9.4
V68W	0.17	0.26	1.5	4.1
L29F/V68F	13	0.17	0.013	2.9
H64F/V68F	13	1700	130	1.8
H64Q/V68F	3.0	12	4.0	7.5
H64Q/V68W	2.6	12	4.6	2.0
L29F/H64Q <sup>b</sup>	30	65	2.2	17
L29W/H64Q	12	67	5.6	3.0
L29F/H64Q/V68I	5.1	79	15	1.5
L29F/H64Q/V68L	61	14	0.23	5.1
L29F/H64Q/V68F <sup>c</sup>	13	3.4	0.26	13

$k'_{\text{NO,ox}}$  is the bimolecular rate constant for NO dioxygenation by MbO<sub>2</sub>. Parameters for the single mutants were taken from the literature [3,14,55]. Parameters for some of the multiple mutants were first reported in Olson et al. [18] and Eich [55].

<sup>a</sup> It has proved difficult to get an accurate value of the rate of NO dioxygenation for Gln64(E7) myoglobin because of the rapid rate of NO binding to the ferric derivative. The value of 60  $\mu\text{M}^{-1} \text{s}^{-1}$  is our current best estimated, based on reactions in which deoxyMb was varied and mixed with sub-stoichiometric amounts of NO.

<sup>b</sup> Elephant Mb has naturally occurring Gln64 and Phe29 residues in its distal pocket [96].

<sup>c</sup> Lucina Hb I contains Gln(E7), Phe(B10), and Phe(E11) residues [97].

for an N-terminal methionine residue. In this system, *E. coli* TB1 cells were used and are missing the gene for the lac repressor protein. The bacteria synthesize the required heme, and the holoprotein is obtained directly from the bacterial cytoplasm. This constitutive expression system only works well with sperm whale myoglobins, which have an unusually stable apoglobin [20]. In the third system, a pET vector is used to overexpress the myoglobin gene containing the starting N-Met codon. Both holoprotein and unfolded apoglobin are made after induction with IPTG. The latter system was first used to make recombinant horse heart myoglobin [13], and similar systems have been developed for labeling sperm whale myoglobin with <sup>13</sup>C and <sup>15</sup>N amino acids.

## 2.2. Kinetics of ligand binding and NO dioxygenation

The new rate constants for the multiple mutants listed in Table 1 were measured as described in previous publications on O<sub>2</sub> and NO binding to deoxymyoglobin [32] and NO induced oxidation [3,33,34]. In general, rate constants for O<sub>2</sub> and NO association are measured on microsecond and milliseconds time scales using room temperature laser photolysis techniques and, when possible, checked in rapid mixing experiments. Oxygen dissociation rate constants are determined by analysis of CO replacement reactions [35]. The equilibrium dissociation constant (listed as  $P_{50}$  in units of  $\mu\text{M}$ ) were calculated from the ratio of the

dissociation,  $k_{O_2}$ , and association,  $k'_{O_2}$ , rate constants (i.e.  $K_d = P_{50} = k_{O_2}/k'_{O_2}$ ).

### 2.3. Mean arterial blood pressure or total peripheral resistance experiments

Blood pressure measurements were taken from the literature (Fig. 5) and are based on work by the research group at Baxter Hemoglobin Therapeutics (formerly Somatogen, [28,29]) and by Winslow, Intaglietta, and coworkers at the University of California, San Diego [36,37]. All experiments were carried out with rats and involved either 10% top load experiments or 40–50% isovolemic exchange, and when possible the data are reported as the change in blood pressure compared to serum albumin controls. In the case of 10% top load experiments, the albumin controls show small  $\sim 5\%$  increases in MAP due to the initial increase blood volume. When controls using human serum albumin (HSA) are carried out for 40–50% isovolemic exchanges, there are significant decreases in both blood pressure ( $\sim 10\%$ ) and peripheral resistance ( $\sim 20\%$ ) [29,37] due to large decreases in blood viscosity. The latter effect could mask the pharmacological activity of the hemoglobin being examined. Unfortunately, Rohlf et al. (1998) did not report serum albumin controls in their 50% exchange experiments and only the uncorrected changes in mean arterial blood pressure are reported in Figs. 5 and 6. Regardless, the data for simple cross-linked hemoglobin tetramers (without distal pocket mutations) show no obvious dependence of the change in mean arterial blood pressure on  $P_{50}$ , in either 10% top load or 40–50% isovolemic exchange experiments (Fig. 6a).

### 2.4. $O_2$ transport

Measurements of  $O_2$  uptake and release by sperm whale myoglobin mutants in a 25  $\mu\text{m}$  diameter artificial capillary were made as described by Page, Hellums, and colleagues in work with bovine hemoglobin and red cells [38–40]. The myoglobin samples were more dilute ( $\sim 0.5$  mM heme) due to the large volume required for these experiments ( $\sim 5$  ml). The lower absolute absorbance values for the Mb samples accounts for the

greater noise in the data shown in Fig. 8. In Page et al.'s [38,40] and our previous measurements [41,42], the Hb concentration was 1–5 mM. Complete descriptions of the 25–30  $\mu\text{m}$  capillary flow system and the microspectrophotometer are given in Boland et al. [41] and Page et al. [38,40]. A 100- $\mu\text{m}$  slab of clear, highly gas permeable silicone rubber is cast around a 20–30  $\mu\text{m}$  tungsten wire. After polymerization, the wire is removed and the input and output sides of the capillary are cannulated with glass micropipettes. The pipette on the input side is connected to a reservoir containing a concentrated Hb or Mb solution. The output side is connected to a syringe pump which draws the sample through the capillary at well-defined flow rates. The silicone wafer is placed on a stage which can be translated with fine precision across the light beam of the microscope. The transmitted light is split into two beams by fiber optic cables and sent to two photomultipliers, which measure absorbance changes at 415 and 430 nm simultaneously. Release experiments are initiated by flowing  $\text{HbO}_2$  or  $\text{MbO}_2$  through the capillary as it is being flushed with  $\text{N}_2$ . In uptake experiments, deoxyHb or deoxyMb is used, and the capillary bed is flushed with air and  $\text{O}_2/\text{N}_2$  mixtures. Absorbance change readings are made at 5 to 10 positions along the length of the capillary and used to calculate fractional degree of saturation. The residence time is calculated from the longitudinal position and the flow rate [38,40].

## 3. Results

### 3.1. Mechanisms for $O_2$ binding

More than 300 mutants have been constructed at 50 different positions in myoglobin. The locations of these mutants are shown in Fig. 1 where the residues are color-coded by their helix position. Many of the mutant proteins have multiple replacements (e.g. Table 1). The substitutions were designed to test mechanisms of ligand binding and to improve the properties of the molecule with respect to  $O_2$  transport, stability, and NO scavenging. A database for the functional and structural properties of these mutants is being

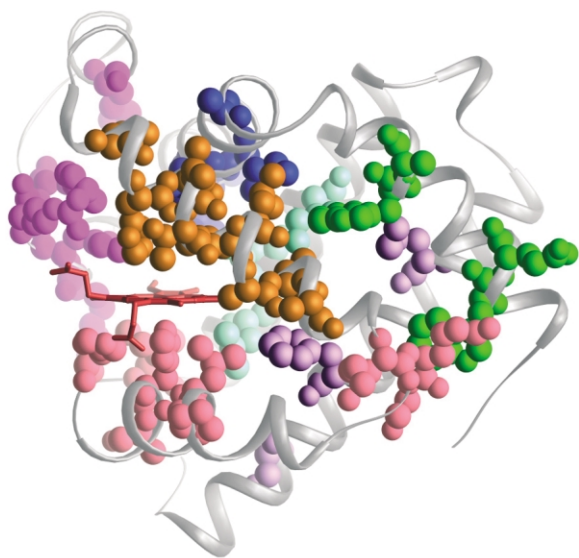


Fig. 1. Structure of sperm whale myoglobin showing the positions that have been mutated and examined. The colors are grouped according to helical positions. Deep green, A-helix; blue, B-helix; bright violet, C- and D-helices and CD corner; orange, E-helix; rose, EF corner, F-helix, and FG corner; light green (background), G-helix; and purple, H-helix. Lists of single mutants are given in various publications and the website.

constructed at <http://olsonnt1.bioc.rice.edu/web/myoglobinhome.asp>.

The structural factors regulating  $O_2$  affinity in both hemoglobins and myoglobins are summarized in Figs. 2 and 3. The reactivity of the heme iron atom can be altered dramatically by stereochemical constraints on the proximal side of the heme group. Large changes in ligand affinity are observed when comparing equilibrium constants for ligand binding to the high affinity (R) and low affinity (T) quaternary states of human hemoglobin. The R to T conformational change causes the E and F helices to restrict the ability of the iron atom to move into the plane of the porphyrin ring and react with ligands [43,44]. As a result, this quaternary transition causes 700, 1200, and 1000-fold decreases in the equilibrium constants for  $O_2$ , CO, and NO binding to human hemoglobin, respectively (see [45,46] and references therein).

In contrast to the proximal effects, electrostatic interactions with polar side chains on the distal side of the heme group selectively regulate  $O_2$

binding [14,45,47]. Amino acids with good hydrogen atom donors (i.e. His, Gln, Asn, Tyr) favor the binding of dioxygen by preferentially stabilizing the highly polar  $Fe^{\delta(+)}-O-O^{\delta(-)}$  complex. We have quantified these effects by assigning values to the equilibrium constants for non-covalent water binding to deoxymyoglobin, ligand entry into the distal pocket, internal coordination to the iron atom, and electrostatic stabilization of the bound ligand [45]. In the case of mammalian myoglobin, the distal His64(E7) side chain forms a strong H-bond that selectively stabilizes bound  $O_2$  by a factor of  $\sim 1000$ .

Maps for  $O_2$  movement into and out of the myoglobin have been constructed based on analyses of time courses for geminate and bimolecular  $O_2$  binding to 90 myoglobin mutants at 27 different positions [48,49]. We have argued that the protein acts as a baseball glove to ‘catch’ and then ‘trap’

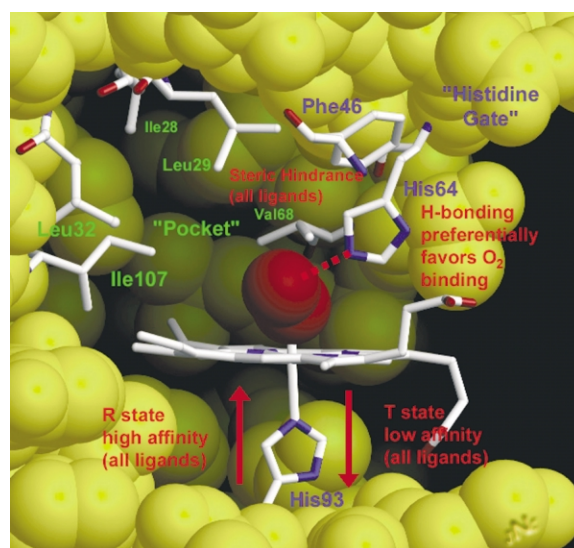


Fig. 2. Regulation of  $O_2$  affinity and CO discrimination in Mb and Hb. The structure of the active side of recombinant sperm whale MbO<sub>2</sub> was taken from Quillin et al. [98]. Schematic chemical drawings of the active site are shown in Fig. 3A,B. The amino acid numbers 28, 29, 32, 46, 64, 68, 93, and 107 correspond to the helical positions, B9, B10, B13, CD4, E7, E11, F8, and G8, respectively. The amino acids labeled in blue comprise the distal histidine gate, and the amino acids labeled in green circumscribe the Xe4 binding site. The factors governing  $O_2$  affinity are labeled in red and taken from Olson and Phillips [45].

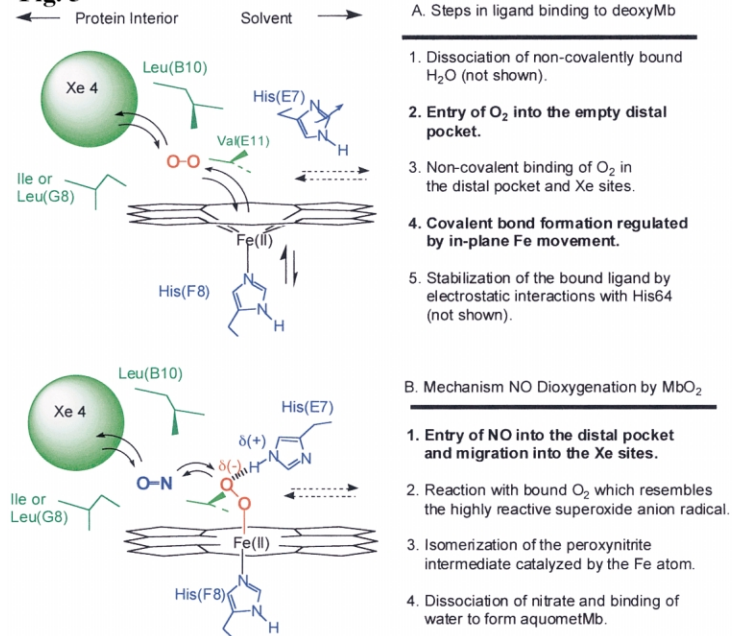
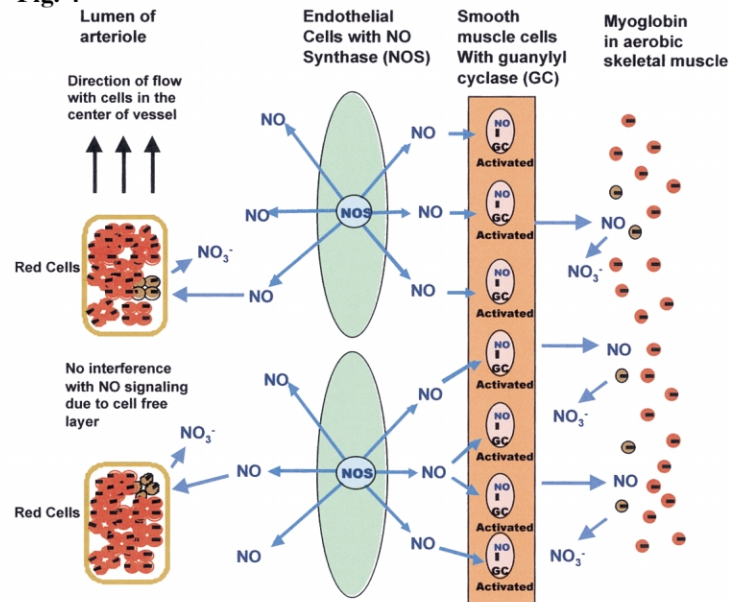
**Fig. 3****Fig. 4**

Fig. 3. Comparison of kinetic pathways for  $\text{O}_2$  binding and NO dioxygenation. The mechanisms were taken from the literature [3,34,45,48]. Oxygen binding can be broken down into five discrete steps and those labeled in bold, ligand entry and bond formation, limit the rate constant for  $\text{O}_2$  association at room temperature. There are four distinct steps for NO dioxygenation. The first step, NO entry into the distal pocket, is rate limiting at neutral pH and room temperature.

Fig. 4. NO signaling in the endothelium and the roles of  $\text{HbO}_2$  and  $\text{MbO}_2$  in detoxifying NO that escapes into the blood stream and muscle tissue. This scheme is based on the ideas developed over the past 5 years on the physiological role of rapid NO dioxygenation by the oxygenated forms hemoglobins and myoglobins [5,6].

incoming ligand molecules long enough to allow bond formation with the iron atom. Opening of the glove occurs by outward movements of the distal histidine. Ligands are captured in the interior ‘webbing’ of the distal pocket, which is circumscribed by residues 28(B9), 29(B10), 32(B13), 68(E11), and 107(G8) (Fig. 2) and includes the Xe4 binding site discovered in Mb crystals equilibrated with xenon gas [50]. The rate constants for ligand capture are reduced if the pocket of the glove is reduced in size with Phe or Trp substitutions at positions 28, 29, 32, 68, and 107 [48].

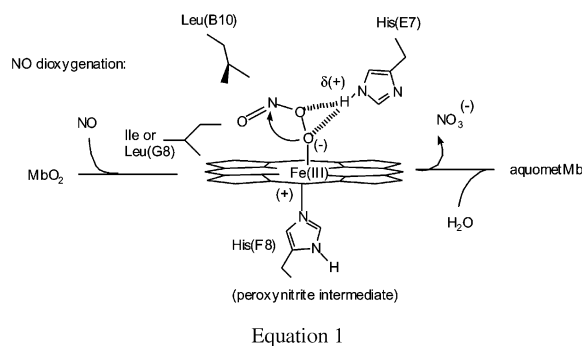
An exception occurs for the Leu29(B10) to Phe mutation where the rate of  $O_2$  binding,  $k'_{O_2}$ , increases  $\sim 25\%$  (Table 1). The large size of the phenyl ring displaces the water molecule that is found attached to the distal His64(E7) residue in native deoxyMb [51]. Loss of distal pocket water by replacement of His(E7) with Leu or Phe causes  $\sim 10$ -fold increases in the rate of  $O_2$  binding (H64F, Table 1). The favorable effect of displacing distal pocket water by Phe(B10) is offset by the inhibition of ligand entry due to the large size of the benzyl side chain. As a result, there is little difference between  $k'_{O_2}$  for Phe(B10) and that for wild-type Mb. The remarkably low value of  $k_{O_2}$  for Phe(B10) is due to favorably electrostatic interactions between bound  $O_2$  and the positive edge of the phenyl multipole [52].

In the Trp29(B10) mutant, the large indole side chain not only fills the distal pocket, but also sterically hinders access to the iron and the bound ligand. The net result for Trp(B10) Mb is a dramatic 100-fold decrease in  $k'_{O_2}$  compared with the wild-type protein (L29W, Table 1). These results point out the unique properties of the B10 residue, which can affect electrostatic interactions with the bound ligand, the size of the distal pocket for ligand capture, and the steric accessibility of the iron atom. Brunori and coworkers have examined the effects of Tyr(B10) mutations in various myoglobin backgrounds that were originally designed to mimic the distal pocket structure of *Ascaris suum* hemoglobin [30,53]. They found that all three effects, pocket size, steric hindrance, and H-bonding, play important roles in regulating ligand binding by the Tyr(B10) side chain [54].

The cavities in the interior of myoglobin are also important for ligand release. These spaces allow the dissociated  $O_2$  molecules to remain unattached to the iron atom long enough for escape out through the distal histidine gate. If these spaces are filled with large residues, the overall rate constants for  $O_2$  dissociation decrease (see V68F, V68W entries Table 1, and Scott et al. [48]).

### 3.2. The mechanism of NO dioxygenation

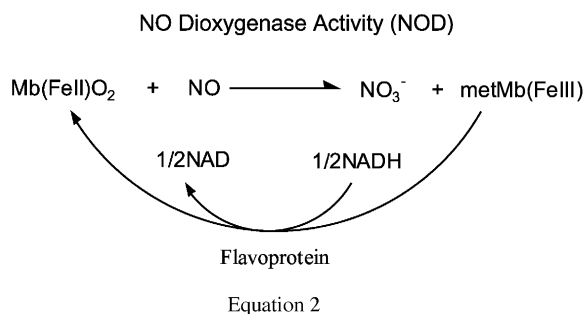
The major NO scavenging reaction in mammals is NO dioxygenation by MbO<sub>2</sub> and HbO<sub>2</sub>, which are the predominant species found in aerobic muscle and in arterial blood. When either MbO<sub>2</sub> or HbO<sub>2</sub> is mixed with NO, the solution changes immediately from red to brown, and this color change has served as a simple assay for NO synthase activity for over 20 years. Before 1995, the only detailed mechanistic study of this reaction was carried out by Doyle and Hoekstra [2]. They showed that NO is rapidly and stoichiometrically converted to NO<sub>3</sub><sup>-</sup> in the presence of oxyhemoglobin. In 1996, Wade and Castro [4] re-examined the stoichiometry of this reaction, and at approximately the same time, we examined the mechanism of NO-induced oxidation by wild type and mutant HbO<sub>2</sub> and MbO<sub>2</sub> [3,18,55]. In the past three years, Herold and coworkers have reported even more definitive kinetic and chemical characterizations of this reaction [33,34]. The mechanism is given in Eq. 1 and Fig. 3B.



At neutral pH, the rate limiting step is bimolec-

ular entry of NO into the distal pocket. The non-covalent capture of NO is followed by rapid reaction with bound oxygen, which resembles superoxide anion (Fig. 3B). The resultant Fe–OONO<sup>−</sup> complex isomerizes to NO<sub>3</sub><sup>−</sup> in an internal, metal catalyzed reaction that is too fast to be detected at pH 7 (i.e.  $\geq \sim 500 \text{ s}^{-1}$ ). Herold and coworkers were able to identify the peroxynitrite intermediate by increasing the pH of the reaction solution to slow the rate of isomerization and to enhance the spectral differences between the intermediate and methemoglobin [33,34]. However, no release of free peroxynitrite was observed at either low or high pH. Herold, Watanabe, and coworkers have shown that H64G and H64A mutants of myoglobin can efficiently catalyze the isomerization of exogenously added ONOO<sup>−</sup> salts [56]. This more recent work confirms that rapid isomerization of peroxynitrite is an intrinsic property of the heme group as long as the large anion can gain access to the iron atom.

In 1998 Paul Gardner [57] discovered that *E. coli* flavohemoglobin catalyzes the oxidation of NO to nitrate by a reaction which is identical to that involved in NO scavenging by HbO<sub>2</sub> and MbO<sub>2</sub>. Gardner named this process NO dioxygenation, which we now prefer to the older term, NO-induced oxidation. Using <sup>15</sup>NO and <sup>18</sup>O<sub>2</sub>, he has shown that both atoms of bound oxygen are incorporated into the nitrate product when the reaction is carried out either by *E. coli* flavoHb or human hemoglobin A [58]. In the case of flavohemoglobin, the ferric form of the protein is rapidly re-reduced by NADH through a flavin-containing reductase domain.



Similar NO dioxygenase (NOD) activities have been observed for Yeast and *Alcaligenes* flavoHbs [57,59,60]. In principle, all hemoglobins and myoglobins have NOD activity (i.e. NO scavenging). The physiological relevance depends on presence and speed of the corresponding reductase activity. For example, Stamler, Goldberg, and coworkers have suggested that *Ascaris suum* Hb serves to scavenge both O<sub>2</sub> and NO in the body wall of this intestinal parasite in order to keep it anaerobic [61]. However, proof will require the discovery and characterization of a cognate, highly active flavoprotein reductase. In vivo, mammalian metMb is rapidly reduced by the cytochrome b<sub>5</sub> flavoprotein reductase system in myocytes, and human metHb is re-reduced by erythrocyte methemoglobin reductase.

Myoglobin serves to detoxify any NO escaping the endothelium/smooth muscle signaling system. Brunori [5,6] has pointed out that this secondary function of myoglobin is needed to prevent inhibition of muscle respiration. Submicromolar levels of NO can irreversibly inhibit aconitase, shutting down the TCA cycle [62], and low levels of NO inhibit cytochrome c oxidase [63]. Moncada and coworkers [64,65] have shown that NO greatly inhibits respiration in blood vessel endothelial and smooth muscle cells, presumably to allow O<sub>2</sub> transport through these tissues without its consumption.

Gladwin et al. [8] have shown that in healthy human volunteers intracellular hemoglobin reacts rapidly and stoichiometrically with inhaled NO to produce metHb and nitrate ( $\sim 80 \mu\text{M}$  increases in blood after 2 h of inhalation of 80 ppm NO). The level of nitrosylHb is small and increases by an amount (1–2  $\mu\text{M}$  HbNO) predictable by the fraction of deoxyHb in blood passing through the lungs. The absolute amount of S-nitroso- $\beta$  93 S-nitrosocysteine is very small initially, 0.2  $\mu\text{M}$ , and only increases to  $\sim 0.4 \mu\text{M}$  [8]. Thus, the NO dioxygenation activity of hemoglobin will rapidly remove and detoxify any NO entering the blood stream, either from signaling pathways, inflammation responses, or inhalation.

A summary of the secondary physiological roles of HbO<sub>2</sub> and MbO<sub>2</sub> in NO detoxification is shown in Fig. 4. This scheme is based on the studies



discussed in the preceding paragraph, our own work on NO dioxygenation reactions, and ideas presented by Brunori, Lancaster, and their coworkers over the past several years [5,6,66,67]. Nitric oxide generated by NO synthase activity in endothelial cells diffuses into adjacent smooth muscle cells and activates guanylyl cyclase causing a cascade of events that leads to relaxation and arterial dilation. This NO also represses respiration in the vessel walls, facilitating O<sub>2</sub> transport through this tissue. Myoglobin serves to scavenge any NO that escapes into muscle tissue, converting it rapidly to nitrate and preventing inhibition of respiration ( $t_{1/2}$  for NO  $\approx$  10  $\mu$ s, when [MbO<sub>2</sub>] is  $\sim$  2 mM [3,5]).

Hemoglobin removes NO from the blood stream by the same reaction. The half-life for free NO in an oxygenated red cell is  $\leq$  1  $\mu$ s because of the high,  $\sim$  20 mM concentration of HbO<sub>2</sub> [3]. The reaction of external NO with red cells is  $\sim$  1000 times slower ( $t_{1/2} \approx$  1 ms) due to unstirred layers surrounding the surface [66]. The rate of consumption of NO in blood vessels is reduced further by cell free plasma layers that form adjacent to the endothelium as the red cells stream in the center of lumen [68]. Thus, during blood flow in vivo, HbO<sub>2</sub> molecules in red cells do not interfere with NO signaling in the vessel walls but will remove excess NO that enters the blood stream either by endogenous synthesis or inhalation. The biochemical and physiological evidence that intracellular hemoglobin acts as an NO scavenger in vivo, converting it to nitrate, is overwhelming and argues strongly against any significant role in NO transport via S-nitrosation as proposed by Stamler's group [69–71].

### 3.3. Designing extracellular hemoglobin-based blood substitutes

The driving force behind all blood substitute research is the need for an unlimited and safe supply of an O<sub>2</sub> delivery fluid for use in emergencies and elective surgeries that would eliminate current problems with supply and storage of donated blood. A large number of reviews and commentaries have been published over the past two years summarizing the clinical progress, efficacy,

and toxicity of blood substitutes [23,24,26]. The first generation Hb-based products were designed to prevent tetramer dissociation, using specific chemical cross-linking, polymerization with aldehydes, or genetic fusion of  $\alpha$  chains, because dimer formation leads to rapid clearance, oxidative stress, and renal damage [72]. Second generation hemoglobin preparations are being developed to address issues of physiological efficacy and to eliminate side effects associated with vasoconstriction.

#### 3.3.1. The hypertensive (pressor) side effect

Although the severity varies, all first generation Hb-based blood substitute products cause an elevation of mean arterial blood pressure, an increase in total peripheral resistance, some gastrointestinal discomfort and loss of motility, and muscle lesions adjacent to capillaries [24–27]. Although a causal relationship with these side effects was not established, Baxter stopped development of their dapsirin cross-linked tetramer product due to adverse clinical outcomes in phase III trauma trials and a safety study of acute ischemic stroke patients [73,74]. Simple genetically stabilized tetramers were also dropped in favor of developing second generation products, when Baxter purchased Somatogen in 1998.

The hypertensive effect reflects interference with vasoregulation. A summary of recent blood pressure measurements in rat models is shown in Figs. 5 and 6. The addition of a 10% top load (on per iron basis) of simple cross-linked human Hb tetramers causes a very rapid,  $\sim$  30 mmHg rise in blood pressure (Fig. 6a; for time courses see [28]). Three theories have been proposed to explain this effect.

**3.3.1.1. Autooxidation and radical formation.** In the early 1990s, Alayash, Cashion, and others suggested that extracellular hemoglobin causes oxidative stress leading to an inflammation-like response [24,75]. There must be some oxidative stress caused by administration of large doses of extracellular hemoglobin since the protein is cleared from the blood stream in 8–24 h, which requires the removal of large amounts of heme and iron. However, it is unlikely that hemoglobin

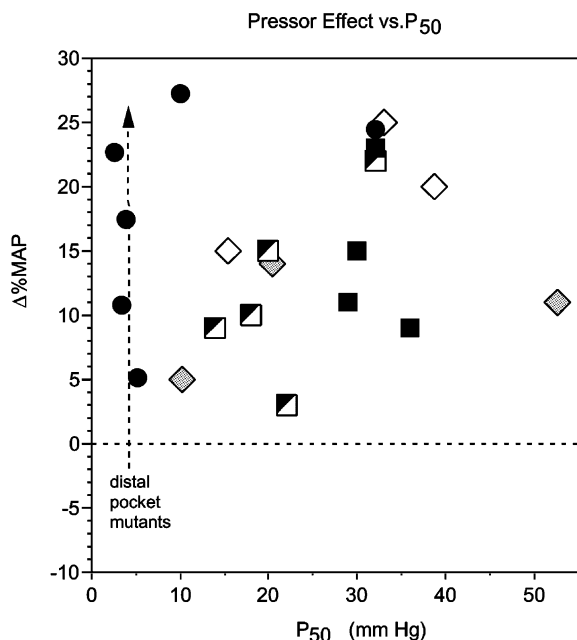


Fig. 5. Lack of dependence of the hypertensive effect on  $P_{50}$ . All experiments were carried out with rats and involved either 10% top load experiments (circles, squares) or 50% isovolemic exchange (diamonds). Symbols: closed circles,  $\Delta\%MAP$  changes compared to HSA controls in 10% top load experiments for 3 rHbs with allosteric mutations to vary  $P_{50}$  and 3 rHbs with distal pocket mutations to reduce NO scavenging [28]. Open diamonds, chemically cross-linked Hb tetramers, and closed diamonds, Hbs decorated with PEG, POE, or  $\alpha$ -poly-rafinosse,  $\Delta\%MAP$  changes in 50% isovolemic exchanges uncorrected for HSA controls [36]. Closed square,  $\Delta\%MAP$  changes compared with HSA controls in 10% top load experiments with glutaraldehyde treated rHb (29). Half-filled squares,  $\Delta\%MAP$  changes compared with HSA controls for polyethylene glycol (PEG)-conjugated Hb, hydroxyethylstarch-conjugated XLHb, polymerized XLHb, and PEG-modified Hb vesicles [37].

oxidation causes the hypertensive effects shown in Fig. 6a. The increase in blood pressure is immediate and occurs seconds to minutes after infusion of extracellular hemoglobin [28,37]. Autooxidation of oxyhemoglobin and subsequent heme loss are much slower processes that occur on time scales of hours to days even in the presence of facilitating anions such as azide or cyanide [21,76,77]. In their most recent work, D'Agnillo and Alayash [78] showed convincingly that simple cross-linked hemoglobin tetramers do react rapidly with low

levels of hydrogen peroxide to form strong oxidants that irreversibly damage endothelial cells. However, there is no evidence that administration of cross-linked or polymerized hemoglobins by themselves cause oxidative stress in control animals or humans which show the blood pressure effect. Most investigators see no evidence for rapid ( $\leq 10$  min) autooxidation of the hemoglobin in vivo [79–81]. Tsuchida's [81] and Chang's [82] groups have incorporated superoxide dismutase and catalase into their blood substitute preparations in efforts to make the hemoglobin molecules more resistant to the oxidative stress associated with reperfusion injury.

**3.3.1.2. Excessive  $O_2$  transport.** Winslow, Intaglietta, and colleagues [23,36,37,83,84] and references therein) have suggested that extracellular hemoglobins are too efficient at transporting oxygen, particularly in small arterioles. They argue that excessive  $O_2$  delivery triggers autoregulatory responses that cause closure of capillary beds by uncontrolled constriction. Extracellular hemoglobins are two to three times more efficient at delivering  $O_2$  than red blood cells [38,39,41] and as a result, Winslow and coworkers have argued that extracellular Hb-based blood substitutes should have low  $P_{50}$  values to limit the amount of oxygen delivered [23,36,83,84].

In our opinion, excess  $O_2$  delivery also does not appear to cause the initial increase in blood pressure. First, the amount of extracellular hemoglobin used in many of the experiments shown in Figs. 5 and 6 is only 10% of the total present and should not have a major impact on oxygen delivery since most of the  $O_2$  transport will be carried out by red cells. Second, there is no obvious dependence of the blood pressure effect on the oxygen transport characteristics of the hemoglobin sample.

A summary of all current data on the blood pressure effect of human hemoglobin preparations in rat models is shown in Fig. 5. The percent change in mean arterial blood pressure is plotted vs. the  $P_{50}$  of the sample. Oxygen delivery in capillaries should be proportional to the  $P_{50}$  of the sample [42,85] (results in Fig. 8a). However, the experimental results for both 10% top load and 40–50% isovolemic exchange show no correlation

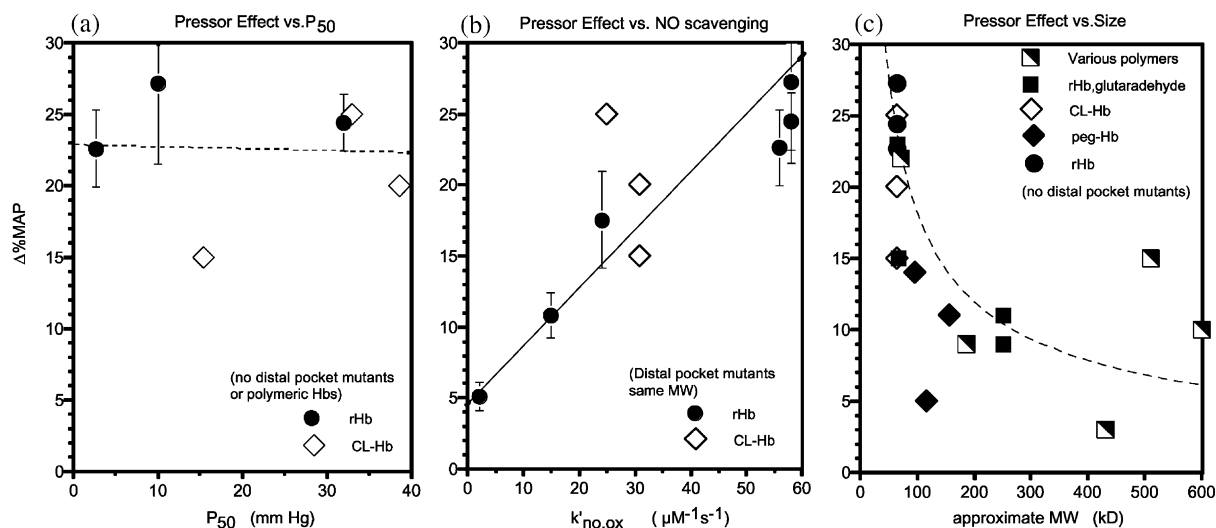


Fig. 6. Dependence of the hypertensive effect on NO scavenging rate and molecular weight. All experiments were carried out with rats and involved either 10% top load experiments (circles, squares) or 50% isovolemic exchange (diamonds). Symbols are the same as in Fig. 5. (a) Effects of  $P_{50}$  on  $\Delta\%MAP$  for a series of simple cross-linked tetramers with very similar rates of NO scavenging; (closed circles)  $\Delta\%MAP$  changes compared with HSA controls in 10% top load experiments for 3 rHbs with allosteric mutations to vary  $P_{50}$  [28], open diamonds, chemically cross-linked Hb tetramers [36]. (b) Effects of  $k'_{NO,ox}$  on  $\Delta\%MAP$  for a series of simple cross-linked tetramers and recombinant hemoglobins with identical sizes but widely different NO scavenging rates; closed circles,  $\Delta\%MAP$  changes compared with HSA controls in 10% top load experiments for 3 rHbs with allosteric mutations to vary  $P_{50}$  and 3 rHbs with distal pocket mutations to reduce NO scavenging [28]; open diamonds, chemically cross-linked Hb tetramers uncorrected for HSA controls [36]. (c) Effects of molecular weight (size) on  $\Delta\%MAP$ ; closed diamonds, Hbs decorated with PEG, POE, or *o*-poly-raffinose,  $\Delta\%MAP$  changes in 50% isovolemic exchanges uncorrected for HSA controls [36]; closed squares,  $\Delta\%MAP$  changes compared to HSA controls in 10% top load experiments with glutaraldehyde treated rHb [29]. Half-filled squares,  $\Delta\%MAP$  changes compared to HSA controls for polyethylene glycol (PEG)-conjugated Hb, hydroxyethylstarch-conjugated XLHb, polymerized XLHb, and PEG-modified Hb vesicles [37].

between the hypertensive effect and oxygen affinity, and initially the data appear scattered and undecipherable. In an attempt to understand these results, the various hemoglobin samples were grouped as simple tetramers with cross-links and modifications that affect  $P_{50}$  by altering the R to T transition, simple tetramers with distal pocket mutations to reduce NO scavenging rates, and polymerized or decorated proteins with increased molecular size. These groupings were used to look individually at the dependence of the pressor effect on: (a)  $P_{50}$  when reactivity with NO and size were kept constant; (b) NO reactivity when size was kept constant; and (c) size when NO reactivity was kept constant (Fig. 6).

As shown in Fig. 6a, there is no dependence of the percent change in mean arterial blood pressure

on the  $P_{50}$  of simple cross-linked tetramers that have the same rate constants for NO scavenging. The data were taken from both the Baxter/Somatogen group [28] and Winslow's group [36], and the range of  $P_{50}$  values is from  $\sim 3$  to 40 mmHg. Doyle et al. [86] reported the same lack of effect of  $P_{50}$  on total peripheral resistance in 40% isovolemic exchange reactions with hemoglobin tetramers showing even lower oxygen affinities. Rohlf et al. [36] suggested that their experimental results show an inverse relationship between  $O_2$  affinity and the pressor response, particularly if the data point at the highest  $P_{50}$  value ( $\sim 50$  mmHg) is neglected (diamonds in Fig. 5). However, when all comparable data in the literature are examined, there is no obvious dependence on  $P_{50}$  (Fig. 5).

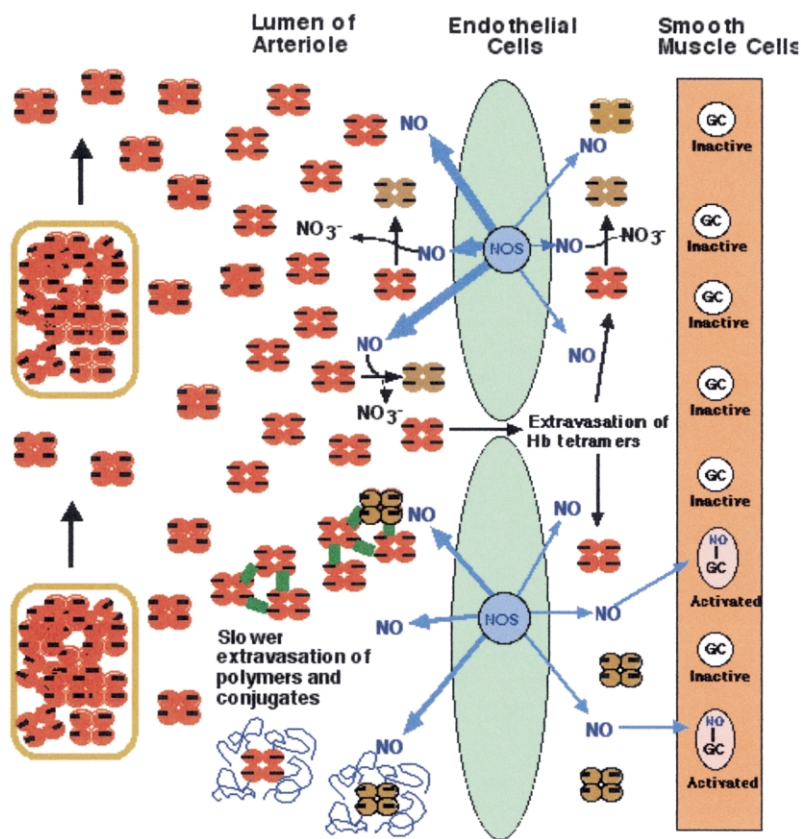


Fig. 7. NO scavenging and its effects on smooth muscle function by extracellular hemoglobin. NO generated by endothelial cells binds to guanylyl cyclase (GC) in the smooth muscles lining arteriole walls, causing a cascade of events that leads to muscle relaxation. Consumption of NO by hemoglobin causes maintenance of the constricted state. DeoxyHb does bind NO rapidly, but oxyHb is the major species present in arterial blood where saturation levels are  $\geq 90\%$ . Thus, the major cause of NO depletion is the oxidative reaction of NO with bound dioxygen. The relative importance of luminal NO scavenging vs. albuminal reactions with extravasated hemoglobin is controversial. At present, most evidence suggests that both reactions affect NO signaling in vivo.

**3.3.1.3. NO scavenging by oxyhemoglobin.** Currently, the most widely accepted interpretation of the hypertensive effect is that extracellular hemoglobin rapidly consumes NO, preventing activation of smooth muscle guanylyl cyclase, subsequent relaxation, and vasodilation of the blood vessel. A model for NO scavenging is shown in Fig. 7 and is based on studies with whole animals, isolated blood vessels, arterial rings, and intestinal cells using extracellular hemoglobin, red blood cells, and NO synthase inhibitors. Liao and coworkers [68] have shown that red blood cells do not interfere significantly with NO gradients when they are streaming through capillaries and presumably

making infrequent contact with the vessel walls. However, all workers have reported contraction of arterial rings and isolated vessels when they are exposed to extracellular hemoglobin, regardless of flow rate [68,87]. The potency of simple stabilized tetramers appears to be increased significantly by rapid extravasation into the spaces between the endothelium and the smooth muscle layer [88].

This model provides simple interpretations of the effects seen by blood substitute products that have been chemically or genetically modified to reduce the hypertensive side effect. Inhibiting the rate of NO dioxygenation by site-directed mutagenesis should decrease interference with NO sig-

naling by allowing NO diffusion to compete effectively with chemical reaction. Doherty et al. [28] showed that there is a strong, linear correlation between the rate of NO dioxygenation measured in vitro and the percent change in mean arterial blood pressure in 10% top load experiments for a series of six distal pocket mutants (Fig. 6b). In more recent work, Doyle et al. [28] have shown a similar linear dependence of the percent change in total peripheral resistance on  $k'_{\text{NO,ox}}$  for distal pocket mutants of human hemoglobin that have  $P_{50}$  values in the range 30–50 mmHg. These results confirm the lack of dependence on  $P_{50}$  when size and reactivity with NO are kept constant. Those molecules that have low reactivity with NO show much reduced pressor effects, regardless of their  $P_{50}$  values.

The gastrointestinal discomfort and motility problems associated with extracellular hemoglobins also appear to be related to NO scavenging and interference with smooth muscle relaxation. The Baxter group has shown that lowering the rate of NO scavenging in recombinant hemoglobin mutants leads to a substantial decrease in this side effect [27]. NO scavenging could also explain the abnormally high rates of  $\text{O}_2$  consumption in microvascular walls that were reported by Intaglietta's group [89] after administration of cell-free hemoglobin. Low levels of free NO are known to inhibit almost completely respiration in endothelial and smooth muscle cells [64]. Scavenging of NO by extracellular  $\text{HbO}_2$  would remove this inhibition, causing  $\text{O}_2$  to be consumed in blood vessel walls rather than transported passively to contracting striated muscle tissue. As pointed out by Tsai et al. [89], the combination of vasoconstriction and premature  $\text{O}_2$  consumption could lead to serious oxygen deficits in actively contracting muscles.

Increasing the size of the Hb-base  $\text{O}_2$  carrier ( $\geq 128\,000$  Da) also causes substantial decreases and almost elimination of the pressor effect as is seen when reactivity NO is reduced  $\geq 30$ -fold (Fig. 6b,c). This effect is seen for glutaraldehyde cross-linked polymers of recombinant hemoglobin [29] and when hemoglobin tetramers are coated with large polyethylene glycol or sugar-like polymers to increase their radius of gyration [36,37]. The underlying cause of the decrease in  $\%\Delta\text{MAP}$

with increasing molecular weight is less clear. We have argued (see Fig. 7) that increasing the radius of the hemoglobin molecule, either by polymerization or decoration with PEG-like molecules, slows the rate of extravasation and inhibits the direct consumption of NO in the spaces between endothelial and smooth muscle cells. If the PEGylated hemoglobins become highly hydrated and interact with each other, they may even tend to stream in the center of the blood vessels and begin to show 'slug' flow in microcapillaries, both of which would inhibit NO scavenging at the lumen wall.

Winslow and coworkers have suggested more complex explanations of the benefits of decoration with polyethers. Their interpretations involve alterations in oncotic pressure, blood viscosity, and  $\text{O}_2$  delivery, all of which must certainly occur for very large PEGylated hemoglobins [23,36,83,84,90]. However, these ideas do not provide an explanation for the effects of mutagenesis on the pressor effects seen for the simple genetically cross-linked tetramers shown in Fig. 6b and those presented in Doyle et al.'s [84] most recent work. In the latter cases, the only structural differences between the samples are internal aromatic amino acid substitutions; all the rheological properties of the hemoglobin preparations are identical. Even though possibly over-simplified, our scheme in Fig. 7 attempts to explain all the size and mutagenesis experiments reported in the literature.

Regardless of the exact mechanism, two basic strategies have been used successfully to reduce NO scavenging and the hypertensive side effect. The first is to keep Hb from extravasating into the endothelium and, if possible, away from the vessel walls by polymerization, PEGylation, or encapsulation into artificial cells. The second is to re-engineer the active site of hemoglobin to inhibit the NO scavenging reaction. Our work has been focused on the basic principles and implementation of the latter protein engineering approach, using recombinant myoglobin as a model system. It is important to note, however, that the chemically simpler strategies of polymerization with glutaraldehyde (strategies adopted by Northfield Laboratories and Biopure, Inc.) and decoration with polyethylene glycol or sugar molecules (strategies

adopted by Hemosal, Ltd. and Sangart, Inc.) have also been successful in reducing the side effects associated with hypertension (Fig. 6c).

### 3.3.2. Strategies for inhibiting the NO scavenging in MbO<sub>2</sub> and HbO<sub>2</sub>

The rate limiting step for NO dioxygenation by MbO<sub>2</sub> is movement of nitric oxide into the protein and capture in the interior of the distal pocket (Figs. 2 and 3B). Thus, one strategy to decrease the rate of NO entry is to reduce the capture volume. Examples of this approach in recombinant sperm whale myoglobin are shown in Table 1. Filling the back of the distal pocket by inserting Phe or Trp residues at the B10 position reduces the rate of NO dioxygenation four- and 10-fold, respectively (Table 1). Similar reductions in  $k'_{\text{NO,ox}}$  are seen for Phe and Trp insertions at the E11 position and to a lesser extent at the G8 position in Mb (data not shown).

Doherty, Mathews, Lemon, and coworkers at Somatogen constructed Phe and Trp replacements at the same three positions in human hemoglobin [3,28]. They discovered that Phe and Trp mutations were most effective at the B10 position in  $\alpha$  subunits and at the E11 and G8 positions in  $\beta$  subunits [3]. We explained these differences between the subunits in terms of the proximity of the native Leu(B10), Val(E11), and Leu(G8) side chains to ligand atoms in the crystal structures of  $\alpha$  and  $\beta$  subunits containing bound ethyl isocyanide. The  $\text{Fe}=\text{C}=\text{N}-\text{CH}_2-\text{CH}_3$  complexes serve as transition state analogues of the non-covalently bound NO intermediate shown in Fig. 3 and the peroxynitrite intermediate shown in Eq. 1 [3].

Using this approach, the Somatogen group constructed a set of four hemoglobins in which the  $k'_{\text{NO,ox}}$  values of the  $\alpha$  and  $\beta$  subunits were matched and progressively decreased from  $\sim 60 \mu\text{M}^{-1} \text{s}^{-1}$  to  $\sim 2 \mu\text{M}^{-1} \text{s}^{-1}$  [28]. As shown in Fig. 6b, there is linear dependence of  $\% \Delta \text{MAP}$  on  $k'_{\text{NO,ox}}$  for this series of test proteins. This result and the lack of dependence on  $P_{50}$  (Fig. 6a) argue strongly that the hypertensive effect is governed by the rate of NO scavenging. In our view, the favorable effects of increased molecular weight or encapsulation are the result of reduced rates of extravasation and perhaps even streaming in the

lumen of the vessel, both of which would reduce interference with NO signaling (Fig. 7). However, the latter interpretation lacks firm experimental support and is speculative.

### 3.3.3. $P_{50}$ and the efficiency of O<sub>2</sub> transport

The initial Mb and Hb mutants constructed to reduce NO dioxygenation have  $P_{50}$  values and oxygen dissociation rate constants that are low enough to cause concern about their efficacy for O<sub>2</sub> transport (see L29F, V68F, and V68W entries, Table 1 [28]). Winslow and others used these initial results to argue that it is impossible to reduce NO scavenging without also increasing O<sub>2</sub> affinity and decreasing the rate of ligand dissociation [83]. Rohlf's et al. [36] argued that the mutagenesis approach would fail since they observed a correlation between NO and O<sub>2</sub> affinities for a series of cross-linked tetramers, polymers, and decorated hemoglobins. However, equilibrium NO binding is not the key parameter for evaluating NO scavenging, which is a kinetic phenomenon that competes with diffusion of the gas to its target in smooth muscle cells. In oxygenated blood substitute preparations, the bimolecular rate constant for NO oxidation to nitrate determines the speed and extent of scavenging compared to signaling. Rohlf's et al.'s [36] data show no correlation between the bimolecular rate constants for NO dioxygenation, which are invariant ( $k'_{\text{NO,ox}} \approx 30 \mu\text{M}^{-1} \text{s}^{-1}$ ), and  $P_{50}$ , which ranges from 10 to 53 mmHg for their samples. To address the problem of  $P_{50}$  vs. NO scavenging, we turned to our library of Mb mutants to obtain a more quantitative understanding of the factors governing O<sub>2</sub> transport and to devise engineering strategies to raise  $P_{50}$  (and  $k_{\text{O}_2}$ ) while keeping  $k'_{\text{NO,ox}}$  small.

Measurements of O<sub>2</sub> uptake and release by recombinant sperm whale myoglobin prototypes were made in a 25  $\mu\text{m}$  capillary system, and the results are shown in Fig. 8. This system was used by Page et al. [38,39] to characterize the transport properties of polymerized bovine hemoglobin preparations that are being developed by for use as blood substitutes by Biopure, Inc. The myoglobin mutants were selected for their widely different oxygen affinities (Table 1). As shown in Fig. 7a, the rate of O<sub>2</sub> release in the capillary depends

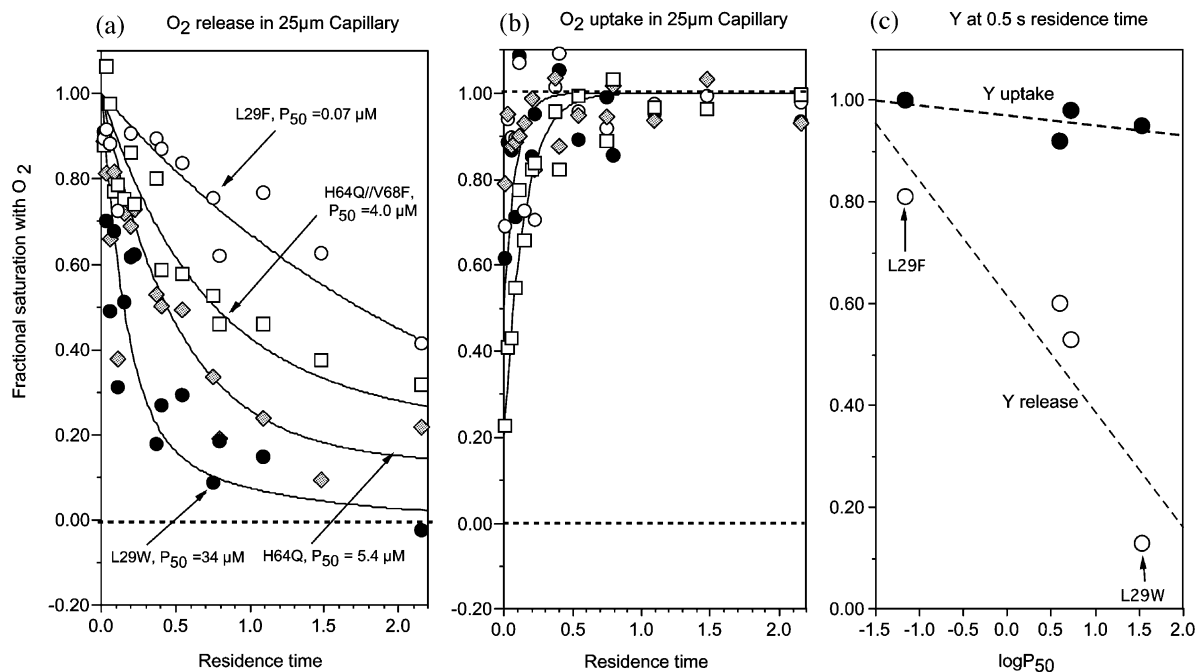


Fig. 8. O<sub>2</sub> release and uptake by Mb mutants during flow through a 25  $\mu\text{m}$  diameter capillary. The residence time is given in seconds. In the release experiments (a), MbO<sub>2</sub> flowed through the lumen while the capillary wafer was continuously flushed with N<sub>2</sub>. In the uptake experiments (b), deoxyMb was sent through the same capillary wafer that was being flushed with humidified air. In (c), the fractional saturation at a residence time of 0.5 s is plotted vs.  $\log(P_{50})$ . Note that for this physiologically relevant resident time, there would be little O<sub>2</sub> delivery from the L29F mutant and almost 100% delivery from the L29W myoglobin. The capillary transport experiments were carried out at 37 °C; the  $P_{50}$  values listed in (a) are for measurements at 20 °C to be consistent with Table 1. For these mutants and wild-type Mb, the  $P_{50}$  values increase by a factor of 3–4 going from 20 to 37 °C [77].

Table 2

Observed vs. Predicted  $P_{50}$  and  $k'_{\text{NO,ox}}$  values for multiple mutants designed as blood substitute prototypes

Multiple mutant	$P_{50}$ ( $\mu\text{M}$ ) observed	$P_{50}$ ( $\mu\text{M}$ ) predicted	$\Delta G_{\text{int}}(P_{50})$ ( $\text{kJ}^{-1} \text{mol}^{-1}$ )	$k'_{\text{NO,ox}}$ ( $\mu\text{M}^{-1} \text{s}^{-1}$ ) observed	$k'_{\text{NO,ox}}$ ( $\mu\text{M}^{-1} \text{s}^{-1}$ ) predicted	$\Delta G_{\text{int}}(k'_{\text{NO,ox}})$ ( $\text{kJ}^{-1} \text{mol}^{-1}$ )
L29F/V68F	<b>0.013</b>	<b>0.16</b>	<b>6.0</b>	2.9	2.2	−0.63
H64F/V68F	130	300	2.0	<b>1.8</b>	<b>17</b>	<b>5.4</b>
H64Q/V68F	4.0	12	2.8	7.5	17	1.9
H64Q/V68W	4.6	8.9	1.6	2.0	7.2	3.1
L29F/H64Q	<b>2.2</b>	<b>0.40</b>	<b>−4.2</b>	17	14	−0.42
L29W/H64Q	<b>5.6</b>	<b>200</b>	<b>8.7</b>	3.0	5.6	1.5
L29F/H64Q/V68I	<b>15</b>	<b>1.9</b>	<b>−5.0</b>	<b>1.5</b>	<b>14</b>	<b>5.4</b>
L29F/H64Q/V68IL	0.23	0.13	−1.4	5.1	10	1.7
L29F/H64Q/V68IF	0.26	0.92	3.0	13	4.0	−2.9

The predicted parameters were calculated from Eq. (4) and the interaction free energy term was computed from Eq. (5). Those parameters with  $|\delta\Delta G_{\text{int}}| \geq 4.0 \text{ kJ mol}^{-1}$  are marked in bold. The results indicate that it is harder to predict  $P_{50}$  values than the rate constant for NO dioxygenation.

directly on the  $P_{50}$  of the myoglobin sample. In contrast, there is little or no dependence of the rate of  $O_2$  uptake on  $P_{50}$  in capillary experiments (Fig. 8b).

These results reflect the diffusion gradients across the capillary wall in the two types of experiments. The gradient is roughly proportional to the difference between  $[O_2]$  in the capillary wall and the free  $[O_2]$  in the lumen [42,85]. At 50% saturation of the Mb solution, the free concentration of  $O_2$  in the lumen  $\approx P_{50}$  of the protein, which is defined as the free  $[O_2]$  at  $Y=0.50$ . In uptake experiments, the partial pressure of  $O_2$  gas in the capillary wall is nearly equal to that in the gas space ( $\sim 150$  mmHg in air) and is much greater than the  $P_{50}$  (0.1–30 mmHg) of the Mb sample. As a result the gradient for uptake at  $\sim 50\%$  saturation is  $(P_{\text{wall}} - P_{50}) \approx P_{\text{wall}}$ . In release experiments, the external  $[O_2]$  is 0 due to flushing with pure  $N_2$  gas, and the gradient for release at 50% desaturation is  $(P_{\text{wall}} - P_{50}) \approx -P_{50}$ .

The magnitude of these effects are shown in Fig. 8c where the change in saturation after a residence time of 0.5 s is plotted vs. the log of the  $P_{50}$  of the myoglobin sample. All of the samples are able to take up  $O_2$  effectively. Even the L29W mutant, which has an  $O_2$  association rate constant  $\approx 0.2 \mu\text{M}^{-1} \text{s}^{-1}$ , was able to take up  $O_2$  in  $\leq 0.5$  s. These results show that the exact value of  $k'_{O_2}$  is much less important than the  $P_{50}$  value of the protein. In the case of release, there is a roughly linear relationship between the amount of  $O_2$  delivered as measured by  $\Delta Y$  and  $\log P_{50}$  [Fig. 7c, (○)]. Clearly, any successful second generation blood substitute candidate should have a high  $P_{50}$  value as well as a low rate of NO dioxygenation.

### 3.3.4. Raising $P_{50}$ and lowering NO scavenging

Solutions to the problem of decoupling  $P_{50}$  and the rate of NO dioxygenation are relatively straightforward and based on the interactions shown in Figs. 2 and 3. Oxygen affinity can be decreased by weakening electrostatic interactions with the polar  $\text{FeO}_2$  complex or sterically hindering the bound ligand. The strength of hydrogen bonding can be reduced by replacing His(E7) with Gln and steric hindrance can be increased by replacing Val(E11) with Ile (Table 1, H64Q and

V68I mutants). Both the Gln(E7) and Ile(E11) replacements have little effect on the rate of ligand capture in the distal pocket as judged by their NO dioxygenation rate constants,  $k'_{\text{NO,ox}}$  in Table 1.

The Leu(B10) to Trp replacement has both effects. NO dioxygenation is reduced  $\sim 10$ -fold by filling the distal pocket with the indole ring, and  $P_{50}$  is increased  $\sim 30$ -fold due to direct steric hindrance with the bound ligand. The major problem with the Trp(B10) mutation is that the rate of  $O_2$  association is reduced dramatically by this combination of effects. Adding the Gln(E7) substitution to Trp(B10) Mb produces a prototype with optimized  $O_2$  binding properties ( $k'_{O_2} = 12 \mu\text{M}^{-1} \text{s}^{-1}$ ,  $k_{O_2} = 67 \text{s}^{-1}$ ) but still a low value for  $k'_{\text{NO,ox}}$ ,  $3 \mu\text{M}^{-1} \text{s}^{-1}$ .

The results in Table 1 demonstrate unambiguously that NO dioxygenation rates can be manipulated independently of  $O_2$  affinity. Different structural features of the active site control these two properties. Ligand entry and the size of the capture volume in the back of the distal pocket govern the rate of NO dioxygenation.  $O_2$  affinity is determined by steric and electrostatic interactions on the distal side of the heme group and the geometry of the heme–His(F8) complex on the proximal side. Distal regulation can be achieved by mutation of residues B10, E7, E11, and G8 (Figs. 2 and 3, Table 1). In the case of hemoglobin, proximal regulation of oxygen affinity can be manipulated by mutations that affect the allosteric transition. This strategy is particularly effective, since replacements that affect the R to T transition are normally located along the subunit interfaces and are far removed from the distal pocket. Thus, NO reactivity can be reduced by distal pocket mutations, whereas  $P_{50}$  can be increased or decreased by allosteric substitutions that are far removed from the heme group but favor the low affinity quaternary conformation [27,28].

In myoglobin, the most dramatic decoupling of NO dioxygenation from  $O_2$  affinity occurs for the L29F/V68F and H64F/V68F double mutants. The  $P_{50}$  values of these myoglobins are  $\sim 0.01$  and  $100 \mu\text{M}$ , respectively, whereas their rates of NO dioxygenation are virtually identical,  $\sim 2 \mu\text{M}^{-1} \text{s}^{-1}$ . The Phe68(E11) side chain markedly decreases the space available for ligand capture, reducing



$k'_{\text{NO,ox}}$  in both mutants [91]. The Phe29(B10) side chain displaces water in the distal pocket of deoxyMb and stabilizes bound  $\text{O}_2$  electrostatically [52]. Both effects enhance  $\text{O}_2$  affinity significantly. The Phe64(E7) mutation causes loss of the favorable hydrogen bonding interaction that normally occurs between bound  $\text{O}_2$  and the native His (E7) side chain, resulting in a dramatic decrease in  $\text{O}_2$  affinity (see H64F and H64F/V68F entries in Table 1). In combination, these strategies allow selective variation of  $\text{O}_2$  affinity over a 10 000-fold range without altering NO scavenging and refute emphatically the criticism that the two processes cannot be decoupled by protein engineering.

## 4. Discussion

### 4.1. Applications to recombinant hemoglobin

The strategies and ideas developed using the myoglobin prototypes listed in Table 1 have been applied successfully to hemoglobin. The research group at Baxter Hemoglobin Therapeutics (formerly Somatogen) has constructed genetically cross-linked recombinant hemoglobins molecules with 30-fold smaller NO dioxygenation rate constants and, at the same time,  $P_{50}$  values  $\approx 65 \mu\text{M}$  at  $37^\circ\text{C}$ . This was achieved by insertion of Gln(E7) and Trp(B10) into  $\alpha$  subunits and Trp(E11) in  $\beta$  subunits [27]. Brunori and coworkers [30] adopted a similar approach. They constructed His(E7) to Gln and Leu(B10) to Tyr mutations in  $\alpha$  and  $\beta$  subunits of human hemoglobin, and the resultant mutant tetramer had a much reduced rate of NO scavenging. Ho and coworkers [92] have constructed a low  $\text{O}_2$  affinity hemoglobin mutant, which contains a Leu(B10) to Phe mutation in  $\alpha$  subunits to confer resistance to auto- and chemical oxidation and an allosteric Asn108 to Gln mutation in  $\beta$  subunits to stabilize the low affinity T quaternary state.

### 4.2. Predicting multiple mutant properties

Multiple mutations are normally required to minimize NO scavenging and maximize  $\text{O}_2$  transport properties (i.e. large  $P_{50}$  values). The design of multiple mutants would be straightforward if

the effects of the individual replacements were additive on a free energy scale. If additivity applies, the free energy change for  $\text{O}_2$  binding to a double mutant ( $\Delta G_{1,2}$ ) could be calculated from the free energy for  $\text{O}_2$  binding to the wild-type protein ( $\Delta G_{\text{wt}}$ ) plus the sum of the differences in the free energy change for  $\text{O}_2$  binding to each mutant (1 and 2) compared with that of the wild-type protein,  $\delta\Delta G_1 + \delta\Delta G_2$  [93]:

$$\Delta G_{1,2} = \Delta G_{\text{wt}} + \delta\Delta G_1 + \delta\Delta G_2 \quad (3)$$

where:

$$\Delta G_{1,2} = -RT \ln K_{1,2}; \quad \Delta G_{\text{wt}} = -RT \ln K_{\text{wt}}$$

$$\delta\Delta G_1 = -RT \ln(K_1/K_{\text{wt}});$$

$$\delta\Delta G_2 = -RT \ln(K_2/K_{\text{wt}})$$

These logarithmic relationships should hold for kinetic as well as equilibrium parameters if an Eyring or Arrhenius-type transition state model applies to the rate process (i.e.  $k = A \exp\{-\Delta G^\ddagger/RT\}$ ). The predicted parameter can be calculated from the parameter ratios if the free energy effects are additive:

$$K_{1,2} \text{ (predict)} = K_{\text{wt}}(K_1/K_{\text{wt}})(K_2/K_{\text{wt}}) \quad (4)$$

If the effects are not additive on a free energy scale, then an additional interaction term,  $\Delta G_{\text{int}}$ , needs to be added to Eq. (3).  $\Delta G_{\text{int}}$  represents the amount of interference or enhancement that occurs when both mutations are present. As pointed out by Wells [93], this term is not easily predicted and normally has to be determined empirically from observed data as:

$$\Delta G_{\text{int}} = -RT \ln\{K_{1,2}(\text{predicted})/K_{1,2}(\text{observed})\} \quad (5)$$

In the case of kinetic parameters, this term may reflect a change in the rate limiting step by the combination of mutations.

Comparisons of observed and predicted values of  $P_{50}$  and  $k'_{\text{NO,ox}}$  for key double and triple myoglobin mutants are presented in Table 2. In those cases where the predictions differ from the observed values by a factor of  $\geq 5$  (i.e.

$|\Delta G_{\text{int}}| \geq 4.0 \text{ kJ mol}^{-1}$ ), the parameters are marked in bold. Two conclusions can be reached from these data and hold for the larger set of data in our library [55]. First, it is easier to predict the rate constant for NO dioxygenation, which is governed only by ligand entry into the protein, than  $\text{O}_2$  affinity, which involves at least five distinct processes (Fig. 3A). Second, there are steric constraints when attempting to reduce NO scavenging by filling the interior portion of the distal pocket with larger amino acid side chains. Combining Phe(B10) with Ile(E11) or Leu(E11) gives a lower than expected value of  $k'_{\text{NO,ox}}$ , suggesting favorable packing in the protein interior. A similar result is obtained for Phe(E7) and Phe(E11) replacements. However, when we constructed multiple Trp and Phe substitutions at the B10, E11, and G8 positions, the rates of NO dioxygenation are much higher than expected; complex heterogeneous kinetic behavior is often observed; and the proteins are generally unstable.

The data in Table 2 demonstrate the need for crystal structures and molecular dynamics simulations to interpret the  $\Delta G_{\text{int}}$  terms and, eventually, to predict them *de novo*. At present, we have general strategies but specific implementation can be difficult. For example, the rate of NO scavenging can be reduced by decreasing the capture volume in the distal pocket, but it is not clear from primary sequence alignments alone which residues should be changed to large amino acids. In human hemoglobin  $\alpha$  chains, the rate of ligand entry is best slowed by substitutions at the B10 but not the E11 position, whereas in  $\beta$  chains the most dramatic decreases in the rate of ligand capture occur for Trp and Phe insertions at the E11 and G8 positions. Myoglobin shows intermediate behavior with positive effects occurring at all three positions. Similar ambiguities occur when trying to regulate steric hindrance of the bound ligand and hydrogen bonding by distal pocket mutants [94]. This kind of problem is particularly severe when trying to mimic the behavior of naturally occurring hemoglobins by small sets of mutations in recombinant mammalian myoglobins. Often the two proteins have significantly different spatial relationships between the position of the

heme iron atom and various helical segments [54,95].

#### 4.3. Optimizing stability as well as function

Although most attention has been focused on reducing NO scavenging and optimizing  $\text{O}_2$  transport, the resistance of recombinant hemoglobin to oxidation, heme loss, and denaturation is equally important if the prototype is to be commercialized. Autooxidation and subsequent heme loss are the principle causes of particulate formation in hemoglobin solutions. Free heme is insoluble and apohemoglobin denatures quickly at temperatures above  $10^\circ\text{C}$ . Apoglobin stability is a key factor in holoprotein production yield during cytoplasmic expression in bacteria. When induction is used, protein synthesis is more rapid than both endogenous heme biosynthesis and the transport of externally added heme. Newly synthesized apoglobin must be able resist denaturation long enough to pair up with its heme cofactor [15,18,20].

Often stability is sacrificed for function, and a dramatic example is the distal histidine found in almost all mammalian myoglobins. For example, the apoprotein of the Phe(E7) Mb mutant is  $\sim 40$  times more resistant to unfolding than wild-type apoMb; the H64F holoprotein is expressed at higher levels in *E. coli*; and the corresponding Phe(E7) deoxyMb is more resistant to acid denaturation [15,19]. In contrast, the H64F mutation causes a dramatic 130-fold decrease in  $\text{O}_2$  affinity (Table 1) and a 30-fold increase in the rate of autooxidation [77], properties that are highly detrimental to the physiological function of myoglobin in myocytes. Keeping a His(E7) side chain in the apolar heme pocket is unfavorable with respect to apoprotein stability. However, the distal histidine is highly conserved because it is required for electrostatic stabilization of bound  $\text{O}_2$  and resistance to autooxidation. Clearly a compromise has evolved to maintain function at the expense of resistance to unfolding.

It is our goal to develop a database that will contain enough information to allow the design of stable recombinant myoglobins and hemoglobins for a wide variety of pharmaceutical and industrial uses. Despite the problems of predicting multiple

mutant behavior, this rational mutagenesis approach has produced recombinant hemoglobin molecules with little or no pressor effect but  $P_{50}$  values capable of efficient transport and maintenance of oxygen consumption in rats after complete isovolemic exchange [86]. One of these molecules is being developed by Baxter Hemoglobin Therapeutics as a safer, second generation blood substitute. Perhaps even more important, this database has led and will continue to lead to the development and testing of key biochemical and biophysical mechanisms of heme protein function.

### Acknowledgments

We would like to dedicate this paper to Maurizio Brunori, whose friendship and scientific collaborations have added both pleasure and insight into our work over the past 30 years. There has been a competition between the Rome group and our and Quentin Gibson's laboratories, which has been fun, honorable, and highly productive in terms of the exchange of students and ideas. Maurizio's wit has added warmth and humor to what can sometimes be a cold and abrasive profession, and he is always able to bring out the best in his colleagues and competitors.

Supported by Robert A. Welch Foundation Grant C-612 (JSO); National Institutes of Health Grants HL47020 (JSO), and GM35649 (JSO), and the W.M. Keck Center for Computational Biology. David H. Maillett and Raymund F. Eich were recipients of predoctoral fellowships from the NIH training grants GM08280 and GM08362, respectively. Yi Dou was the recipient of a Welch Foundation Postdoctoral Fellowship.

### References

- [1] A. Verma, D.J. Hirsch, C.E. Glatt, G.V. Ronnett, S.H. Snyder, Carbon monoxide: a putative neural messenger, *Science* 259 (1993) 381–384.
- [2] M.P. Doyle, J.W. Hoekstra, Oxidation of nitrogen oxides by bound dioxygen in hemoproteins, *J. Inorg. Biochem.* 14 (1981) 351–358.
- [3] R.F. Eich, T. Li, D.D. Lemon, et al., Mechanism of NO-induced oxidation of myoglobin and hemoglobin, *Biochemistry* 35 (1996) 6976–6983.
- [4] R.S. Wade, C.E. Castro, Reactions of oxymyoglobin with NO, NO<sub>2</sub>, and NO<sub>2</sub><sup>-</sup> under argon and in air, *Chem. Res. Toxicol.* 9 (1996) 1382–1390.
- [5] M. Brunori, Nitric oxide moves myoglobin centre stage, *Trends Biochem. Sci.* 26 (2001) 209–210.
- [6] M. Brunori, Nitric oxide, cytochrome-c oxidase and myoglobin, *Trends Biochem. Sci.* 26 (2001) 21–23.
- [7] P. Ascenzi, M. Brunori, Myoglobin: a pseudo-enzymatic scavenger of nitric oxide, *Biochem. Mol. Biol. Educ.* 29 (2001) 183–185.
- [8] M.T. Gladwin, F.P. Ognibene, L.K. Pannell, et al., Relative role of heme nitrosylation and beta-cysteine 93 nitrosation in the transport and metabolism of nitric oxide by hemoglobin in the human circulation, *Proc. Natl. Acad. Sci. USA* 97 (2000) 9943–9948.
- [9] K. Nagai, M.F. Perutz, C. Poyart, Oxygen binding properties of human mutant hemoglobins synthesized in *Escherichia coli*, *Proc. Natl. Acad. Sci. USA* 82 (1985) 7252–7255.
- [10] R. Varadarajan, A. Szabo, S.G. Boxer, Cloning, expression in *Escherichia coli*, and reconstitution of human myoglobin, *Proc. Natl. Acad. Sci. USA* 82 (1985) 5681–5684.
- [11] B.A. Springer, S.G. Sligar, High-level expression of sperm whale myoglobin in *Escherichia coli*, *Proc. Natl. Acad. Sci. USA* 84 (1987) 8961–8965.
- [12] G. Dodson, R.E. Hubbard, T.J. Oldfield, S.J. Smerdon, A.J. Wilkinson, Apomyoglobin as a molecular recognition surface: expression, reconstitution and crystallization of recombinant porcine myoglobin in *Escherichia coli*, *Protein Eng.* 2 (1988) 233–237.
- [13] E. Lloyd, A.G. Mauk, Formation of sulphmyoglobin during expression of horse heart myoglobin in *Escherichia coli*, *FEBS Lett* 340 (1994) 281–286.
- [14] B.A. Springer, S.G. Sligar, J.S. Olson, G.N. Phillips, Mechanisms of ligand recognition in myoglobin, *Chem. Rev.* 94 (1994) 699–714.
- [15] M.S. Hargrove, S. Krzywdka, A.J. Wilkinson, Y. Dou, M. Ikeda-Saito, J.S. Olson, Stability of myoglobin: a model for the folding of heme proteins, *Biochemistry* 33 (1994) 11767–11775.
- [16] T.L. Whitaker, M.B. Berry, E.L. Ho, et al., The D-helix in myoglobin and in the beta subunit of hemoglobin is required for the retention of heme [published erratum appears in *Biochemistry* 1997;36(38):15542], *Biochemistry* 34 (1995) 8221–8226.
- [17] M.S. Hargrove, A.J. Wilkinson, J.S. Olson, Structural factors governing heme dissociation from metmyoglobin, *Biochemistry* 35 (1996) 11300–11309.
- [18] J.S. Olson, R.F. Eich, L.P. Smith, J.J. Warren, B.C. Knowles, Protein engineering strategies for designing more stable hemoglobin-based blood substitutes, *Artif. Cells Blood Substit. Immobil. Biotechnol.* 25 (1997) 227–241.
- [19] Q. Tang, W.A. Kalsbeck, J.S. Olson, D.F. Bocian, Disruption of the heme iron-proximal histidine bond

- requires unfolding of deoxymyoglobin, *Biochemistry* 37 (1998) 7047–7056.
- [20] E.E. Scott, E.V. Paster, J.S. Olson, The stabilities of mammalian apomyoglobins vary over a 600-fold range and can be enhanced by comparative mutagenesis, *J. Biol. Chem.* 275 (2000) 27129–27136.
  - [21] M.S. Hargrove, E.W. Singleton, M.L. Quillin, et al., His64(E7)→Tyr apomyoglobin as a reagent for measuring rates of hemin dissociation, *J. Biol. Chem.* 269 (1994) 4207–4214.
  - [22] C.L. Hunter, A.G. Mauk, D.J. Douglas, Dissociation of heme from myoglobin and cytochrome b5: comparison of behavior in solution and the gas phase, *Biochemistry* 36 (1997) 1018–1025.
  - [23] R.M. Winslow, New transfusion strategies: red cell substitutes, *Annu. Rev. Med.* 50 (1999) 337–353.
  - [24] A.I. Alayash, Hemoglobin-based blood substitutes and the hazards of blood radicals, *Free Rad. Res.* (2000) in press.
  - [25] J.R. Hess, Blood substitutes for surgery and trauma: efficacy and toxicity issues, *BioDrugs* 12 (1999) 81–91.
  - [26] A. Gulati, A. Barve, A.P. Sen, Pharmacology of hemoglobin therapeutics, *J. Lab. Clin. Med.* 133 (1999) 112–119.
  - [27] J.C. Hartman, G. Argoudelis, D. Doherty, D. Lemon, R. Gorczynski, Reduced nitric oxide reactivity of a new recombinant human hemoglobin attenuates gastric dysmotility, *Eur. J. Pharmacol.* 363 (1998) 175–178.
  - [28] D.H. Doherty, M.P. Doyle, S.R. Curry, et al., Rate of reaction with nitric oxide determines the hypertensive effect of cell-free hemoglobin, *Nat. Biotechnol.* 16 (1998) 672–676.
  - [29] M.P. Doyle, I. Apostol, B.A. Kerwin, Glutaraldehyde modification of recombinant human hemoglobin alters its hemodynamic properties, *J. Biol. Chem.* 274 (1999) 2583–2591.
  - [30] A.E. Miele, S. Santanch, C. Travaglini-Allocatelli, B. Vallone, M. Brunori, A. Bellelli, Modulation of ligand binding in engineered human hemoglobin distal pocket, *J. Mol. Biol.* 290 (1999) 515–524.
  - [31] Y. Dou, S.J. Admiraal, M. Ikeda-Saito, et al., Alteration of axial coordination by protein engineering in myoglobin. Bisimidazole ligation in the His64→Val/Val68→His double mutant, *J. Biol. Chem.* 270 (1995) 15993–16001.
  - [32] R.J. Rohlfs, A.J. Mathews, T.E. Carver, et al., The effects of amino acid substitution at position E7 (residue 64) on the kinetics of ligand binding to sperm whale myoglobin, *J. Biol. Chem.* 265 (1990) 3168–3176.
  - [33] S. Herold, Kinetic and spectroscopic characterization of an intermediate peroxynitrite complex in the nitrogen monoxide induced oxidation of oxyhemoglobin [corrected and republished article originally printed in *FEBS Lett.* 1998;439(1/2):85–88], *FEBS Lett.* 443 (1999) 81–84.
  - [34] S. Herold, M. Exner, T. Nauser, Kinetic and mechanistic studies of the NO\*-mediated oxidation of oxymyoglobin and oxyhemoglobin, *Biochemistry* 40 (2001) 3385–3395.
  - [35] J.S. Olson, Stopped-flow, rapid mixing measurements of ligand binding to hemoglobin and red cells, *Methods Enzymol.* 76 (1981) 631–651.
  - [36] R.J. Rohlfs, E. Bruner, A. Chiu, et al., Arterial blood pressure responses to cell-free hemoglobin solutions and the reaction with nitric oxide, *J. Biol. Chem.* 273 (1998) 12128–12134.
  - [37] H. Sakai, H. Hara, M. Yuasa, et al., Molecular dimensions of Hb-based O(2) carriers determine constriction of resistance arteries and hypertension, *Am. J. Physiol. Heart Circ. Physiol.* 279 (2000) H908–H915.
  - [38] T.C. Page, W.R. Light, J.D. Hellums, Prediction of microcirculatory oxygen transport by erythrocyte/hemoglobin solution mixtures, *Microvasc. Res.* 56 (1998) 113–126.
  - [39] T.C. Page, W.R. Light, C.B. McKay, J.D. Hellums, Oxygen transport by erythrocyte/hemoglobin solution mixtures in an in vitro capillary as a model of hemoglobin-based oxygen carrier performance, *Microvasc. Res.* 55 (1998) 54–64.
  - [40] T.C. Page, Oxygen transport by erythrocyte/hemoglobin solution mixtures in an in vitro capillary, Department of Chemical Engineering, Rice University, Houston, 1997.
  - [41] E.J. Boland, P.K. Nair, D.D. Lemon, J.S. Olson, J.D. Hellums, An in vitro capillary system for studies on microcirculatory O<sub>2</sub> transport, *J. Appl. Physiol.* 62 (1987) 791–797.
  - [42] D.D. Lemon, P.K. Nair, E.J. Boland, J.S. Olson, J.D. Hellums, Physiological factors affecting O<sub>2</sub> transport by hemoglobin in an in vitro capillary system, *J. Appl. Physiol.* 62 (1987) 798–806.
  - [43] M.F. Perutz, Stereochemistry of cooperative effects in haemoglobin, *Nature* 228 (1970) 726–739.
  - [44] M.F. Perutz, Mechanisms regulating the reactions of human hemoglobin with oxygen and carbon monoxide, *Annu. Rev. Physiol.* 52 (1990) 1–25.
  - [45] J.S. Olson, G.N. Phillips, Myoglobin discriminates between O<sub>2</sub>, NO, and CO by electrostatic interactions with the bound ligand, *J. Biol. Inorg. Chem.* 2 (1997) 544–552.
  - [46] S. Unzai, R. Eich, N. Shibayama, J.S. Olson, H. Morimoto, Rate constants for O<sub>2</sub> and CO binding to the alpha and beta subunits within the R and T states of human hemoglobin, *J. Biol. Chem.* 273 (1998) 23150–23159.
  - [47] G.N. Phillips, M. Teodoro, T. Li, B. Smith, M.M. Gilson, J.S. Olson, Bound CO is a molecular probe of electrostatic potential in the distal pocket of myoglobin, *J. Phys. Chem. B.* 103 (1999) 8817–8829.
  - [48] E.E. Scott, Q.H. Gibson, J.S. Olson, Mapping the pathways for O<sub>2</sub> entry into and exit from myoglobin, *J. Biol. Chem.* 276 (2001) 5177–5188.

- [49] E.E. Scott, Q.H. Gibson, Ligand migration in sperm whale myoglobin, *Biochemistry* 36 (1997) 11909–11917.
- [50] R.F. Tilton, I.D. Kuntz, G.A. Petsko, Cavities in proteins: structure of a metmyoglobin–xenon complex solved to 1.9 Å, *Biochemistry* 23 (1984) 2849–2857.
- [51] M.L. Quillin, Crystal structures of distal pocket mutants of myoglobin, *Biochemistry & Cell Biology*, Rice University, Houston, 1995.
- [52] T.E. Carver, R.E. Brantley, E.W. Singleton, et al., A novel site-directed mutant of myoglobin with an unusually high O<sub>2</sub> affinity and low autooxidation rate, *J. Biol. Chem.* 267 (1992) 14443–14450.
- [53] M. Brunori, F. Cutruzzola, C. Savino, C. Travaglini-Allocatelli, B. Vallone, Q.H. Gibson, Structural dynamics of ligand diffusion in the protein matrix: a study on a new myoglobin mutant Y(B10) Q(E7) R(E10), *Biophys. J.* 76 (1999) 1259–1269.
- [54] F. Draghi, A.F. Miele, C. Travaglini-Allocatelli, et al., Controlling ligand binding in myoglobin by mutagenesis, *J. Biol. Chem.* 277 (2001) 7509–7519.
- [55] R.F. Eich, Reactions of nitric oxide with myoglobin, *Biochemistry & Cell Biology*, Rice University, Houston, TX, 1997.
- [56] S. Herold, T. Matsui, Y. Watanabe, Peroxynitrite isomerization catalyzed by his64 myoglobin mutants, *J. Am. Chem. Soc.* 123 (2001) 4085–4086.
- [57] P.R. Gardner, A.M. Gardner, L.A. Martin, A.L. Salzman, Nitric oxide dioxygenase: an enzymic function for flavohemoglobin, *Proc. Natl. Acad. Sci. USA* 95 (1998) 10378–10383.
- [58] A.M. Gardner, P.R. Gardner, W. Brashear, K.D.R. Setchell, J.S. Olson, Fidelity of O-atom transfer in the mechanism of nitric oxide dioxygenation by oxy-hemoglobins [Abstr.] (2001) submitted.
- [59] P.R. Gardner, A.M. Gardner, L.A. Martin, et al., Nitric oxide dioxygenase activity and function of flavohemoglobins. Sensitivity to nitric oxide and carbon monoxide inhibition, *J. Biol. Chem.* 275 (2000) 31581–31587.
- [60] A.M. Gardner, L.A. Martin, P.R. Gardner, Y. Dou, J.S. Olson, Steady-state and transient kinetics of *Escherichia coli* nitric-oxide dioxygenase (flavohemoglobin). The B10 tyrosine hydroxyl is essential for dioxygen binding and catalysis, *J. Biol. Chem.* 275 (2000) 12581–12589.
- [61] D.M. Minning, A.J. Gow, J. Bonaventura, R. Braun, M. Dewhirst, D.E. Goldberg, J.S. Stamler, Ascaris haemoglobin is a nitric oxide-activated 'deoxygenase' [see comments], *Nature* 401 (1999) 497–502.
- [62] P.R. Gardner, G. Costantino, A.L. Salzman, Constitutive and adaptive detoxification of nitric oxide in *Escherichia coli*. Role of nitric-oxide dioxygenase in the protection of aconitase, *J. Biol. Chem.* 273 (1998) 26528–26533.
- [63] P. Sarti, A. Giuffrè, E. Forte, D. Mastronicola, M.C. Barone, M. Brunori, Nitric oxide and cytochrome c oxidase: mechanisms of inhibition and NO degradation, *Biochem. Biophys. Res. Commun.* 274 (2000) 183–187.
- [64] E. Clementi, G.C. Brown, N. Foxwell, S. Moncada, On the mechanism by which vascular endothelial cells regulate their oxygen consumption, *Proc Natl Acad Sci USA* 96 (1999) 1559–1562.
- [65] E. Clementi, G.C. Brown, M. Feelisch, S. Moncada, Persistent inhibition of cell respiration by nitric oxide: crucial role of S-nitrosylation of mitochondrial complex I and protective action of glutathione, *Proc Natl Acad Sci USA* 95 (1998) 7631–7636.
- [66] X. Liu, M.J. Miller, M.S. Joshi, H. Sadowska-Krowicka, D.A. Clark, J.R. Lancaster, Diffusion-limited reaction of free nitric oxide with erythrocytes, *J. Biol. Chem.* 273 (1998) 18709–18713.
- [67] D.D. Thomas, X. Liu, S.P. Kantrow, J.R. Lancaster, The biological lifetime of nitric oxide: implications for the perivascular dynamics of NO and O<sub>2</sub>, *Proc. Natl. Acad. Sci. USA* 98 (2001) 355–360.
- [68] J.C. Liao, M.W. Vaughn, K.T. Huang, L. Kuo, Intravascular flow decreases erythrocyte consumption of nitric oxide, *Proc. Natl. Acad. Sci. USA* 96 (1999) 8757–8761.
- [69] L. Jia, C. Bonaventura, J. Bonaventura, J.S. Stamler, S-Nitrosohaemoglobin: a dynamic activity of blood involved in vascular control [see comments], *Nature* 380 (1996) 221–226.
- [70] J.S. Stamler, L. Jia, J.P. Eu, et al., Blood flow regulation by S-nitrosohemoglobin in the physiological oxygen gradient, *Science* 276 (1997) 2034–2037.
- [71] J.R. Pawloski, D.T. Hess, J.S. Stamler, Export by red blood cells of nitric oxide bioactivity, *Nature* 409 (2001) 622–626.
- [72] T.M.S. Chang, Blood Substitutes: Principles, Methods, Products and Clinical Trials, 1., Karger-Landes, Basel, 1997.
- [73] E.R. Sloan, M. Koenigsberg, D. Gens, et al., Disapirin cross-linked hemoglobin (DCLHb) in the treatment of severe traumatic hemorrhagic shock: a randomized controlled efficacy trial, *J. Am. Med. Assoc.* 282 (1999) 1857–1864.
- [74] R. Saxena, A.D. Wijnhou, H. Carton, et al., Controlled safety study of a hemoglobin-based oxygen carrier, DCLHb, in acute ischemic stroke, *Stroke* 30 (1999) 993–996.
- [75] A.I. Alayash, R.E. Cashion, Hemoglobin and free radicals: implications for the development of a safe blood substitute, *Mol. Med. Today* 1 (1995) 122–127.
- [76] M.S. Hargrove, T. Whitaker, J.S. Olson, R.J. Vali, A.J. Mathews, Quaternary structure regulates heme dissociation from human hemoglobin [published erratum appears in *J Biol Chem* 1997;272(38):24096], *J. Biol. Chem.* 272 (1997) 17385–17389.
- [77] R.E. Brantley, S.J. Smerdon, A.J. Wilkinson, E.W. Singleton, J.S. Olson, The mechanism of autooxidation of myoglobin, *J. Biol. Chem.* 268 (1993) 6995–7010.
- [78] F. D'Agnillo, A.I. Alayash, Redox cycling of diaspirin cross-linked hemoglobin induces G2/M arrest and apop-

- tosis in cultured endothelial cells, *Blood* 98 (2001) 3315–3323.
- [79] G.S. Hughes, V.L. DeSmith, P.K. Locker, S.F. Francom, Phlebotomy of 500 or 750 milliliters of whole blood followed by isovolemic hemodilution or autologous transfusion yields similar hemodynamic, hematologic, and biochemical effects, *J. Lab. Clin. Med.* 123 (1994) 290–298.
- [80] G.S. Hughes, E.J. Antal, P.K. Locker, S.F. Francom, W.J. Adams, E.E. Jacobs, Physiology and pharmacokinetics of a novel hemoglobin-based oxygen carrier in humans, *Crit. Care Med.* 24 (1996) 756–764.
- [81] S. Takeoka, T.S.H. Ohgushi, T. Kose, H. Nishde, E. Tsuchida, Construction of artificial methemoglobin reduction systems in Hb vesicles, *Art. Cells Blood Subs. Immob. Biotech.* 25 (1997) 31–41.
- [82] F. D'Agnillo, T.M. Chang, Polyhemoglobin-superoxide dismutase-catalase as a blood substitute with antioxidant properties [see comments], *Nat. Biotechnol.* 16 (1998) 667–671.
- [83] R.M. Winslow, Artificial blood: ancient dream, modern enigma [news; comment], *Nat. Biotechnol.* 16 (1998) 621–622.
- [84] M.R. McCarthy, K.D. Vandegriff, R.M. Winslow, The role of facilitated diffusion in oxygen transport by cell-free hemoglobins: implications for the design of hemoglobin-based oxygen carriers, *Biophys. Chem.* 92 (2001) 103–117.
- [85] P.K. Nair, J.D. Hellums, J.S. Olson, Prediction of oxygen transport rates in blood flowing in large capillaries, *Microvasc. Res.* 38 (1989) 269–285.
- [86] M.P. Doyle, M.D. Cassens, D.H. Doherty, D.D. Lemon, Lowered nitric oxide reactivity decreases vasoconstriction induced by recombinant human hemoglobin [Abstr. presentation], *Artif. Cells Blood Sub. Immobil. Biotech.* 29 (2001) 100.
- [87] M. Wolzt, R.J. MacAllister, D. Davis, et al., Biochemical characterization of S-nitrosohemoglobin. Mechanisms underlying synthesis, no release, and biological activity, *J. Biol. Chem.* 274 (1999) 28983–28990.
- [88] A.L. Baldwin, Modified hemoglobins produce venular interendothelial gaps and albumin leakage in the rat mesentery, *Am J Physiol* 277 (1999) H650–H659.
- [89] A.G. Tsai, H. Kerger, M. Intaglietta, Microvascular oxygen distribution: effects due to free hemoglobin in plasma, in: R.D. Winslow, K.D. Vandegriff, M. Intaglietta (Eds.), *Blood Substitutes: New Challenges*, Birkhauser, Boston, 1996, pp. 124–131.
- [90] R.M. Winslow, A. Gonzales, M.L. Gonzales, et al., Vascular resistance and the efficacy of red cell substitutes in a rat hemorrhage model, *J. Appl. Physiol.* 85 (1998) 993–1003.
- [91] M.L. Quillin, T. Li, J.S. Olson, et al., Structural and functional effects of apolar mutations of the distal valine in myoglobin, *J. Mol. Biol.* 245 (1995) 416–436.
- [92] C.H. Tsai, T.Y. Fang, N.T. Ho, C. Ho, Novel recombinant hemoglobin, rHb (beta N108Q), with low oxygen affinity, high cooperativity, and stability against autoxidation, *Biochemistry* 39 (2000) 13719–13729.
- [93] J.A. Wells, Additivity of mutational effects in proteins, *Biochemistry* 29 (1990) 8509–8517.
- [94] A.J. Mathews, R.J. Rohlfs, J.S. Olson, J. Tame, J.P. Renaud, K. Nagai, The effects of E7 and E11 mutations on the kinetics of ligand binding to R state human hemoglobin, *J. Biol. Chem.* 264 (1989) 16573–16583.
- [95] S.J. Smerdon, S. Krzywda, A.M. Brzozowski, et al., Interactions among residues CD3, E7, E10, and E11 in myoglobins: Attempts to simulate the ligand binding properties of Aplysia myoglobin, *Biochemistry* 34 (1995) 8715–8725.
- [96] X. Zhao, K. Vyas, B.D. Nguyen, et al., A double mutant of sperm whale myoglobin mimics the structure and function of elephant myoglobin, *J. Biol. Chem.* 270 (1995) 20763–20774.
- [97] B.D. Nguyen, X. Zhao, K. Vyas, et al., Solution and crystal structures of a sperm whale myoglobin triple mutant that mimics the sulfide-binding hemoglobin from *Lucina pectinata*, *J. Biol. Chem.* 273 (1998) 9517–9526.
- [98] M.L. Quillin, R.M. Arduini, J.S. Olson, G.N. Phillips, High-resolution crystal structures of distal histidine mutants of sperm whale myoglobin, *J. Mol. Biol.* 234 (1993) 140–155.